TCAD Simulations of Radiation Damage in 4H-SiC[⋆]

Jürgen Burin[a,*], Christopher Hahn[a], Philipp Gaggl[a], Andreas Gsponer[a], Simon Waid[a], Thomas Bergauer[a]

[a] *Institute of High Energy Physics, Austrian Academy of Sciences, Nikolsdorfer Gasse 18, Vienna, 1050, Vienna, Austria*

Abstract

In this paper we present simulation based radiation damage modeling of 4H silicon carbide (SiC) using the technology computer aided design (TCAD) tools for up to 1 kV forward and backward bias. After verifying the TCAD framework from Global TCAD Solutions (GTS) against Sentaurus simulations for silicon we use it to approximate measurements of neutron-irradiated 4H-SiC particle detectors, i.e., pin-diodes. Based on our simulations we are not only able to evaluate the accuracy of the predictions but also to provide an explanation for the almost negligible current of radiated devices under high forward bias.

Keywords: TCAD simulations, 4H silicon carbide (SiC), particle detector, radiation damage

1. Introduction

Particle accelerators play a crucial role in exploring the limits of the standard model of physics. In order to develop proper extensions, scientists use information that is gathered from very rare particle collision events. To improve the scientific output of experiments, the luminosity of future colliders, like the Future Circular Collider (FCC) at CERN, will be increased significantly. Such high particle fluxes, which are nowadays already encountered in medical accelerators, lead to more radiation damage in the detectors. In

[⋆] This work was supported by the Austrian Research Promotion Agency (FFG) in the project RadHardDetSim (895291).

[*] corresponding author

Email address: `juergen.burin@oeaw.ac.at` (Jürgen Burin)

order to avoid frequent replacements and a performance loss during operation, materials that feature an improved radiation hardness and can be used to build particle detectors are highly desired. One very promising candidate is silicon carbide (SiC). Due to its wide band gap (low leakage current) and high charge carrier mobility novel devices can be built that outperform their existing silicon based counterparts.

The key question in using SiC, or more specifically the most commonly used polytype 4H-SiC, for high energy physics experiments is in which degree the performance degrades while being exposed to ionizing radiation. Recent measurements [1] revealed that at fluences higher than $10^{15}\,\mathrm{n_{eq}/cm^2}$ the capacitance of a diode is absolutely constant for a bias of $-1\,\mathrm{kV}$ to $1\,\mathrm{kV}$ (see Fig. 4a). Furthermore, it is possible to heavily forward bias the device without seeing significant conduction (see Fig. 5a). In order to understand these observations, technology computer aided design (TCAD) simulations can be beneficial. In the past the latter have been used to describe the degradation of SiC Schottky diodes [2, 3] or neutron detectors using only a single defect [4]. Only recently, a more elaborate model has been proposed to describe the radiation damage within 4H-SiC pin-diodes [5], however, no comprehensive simulations have been conducted yet.

In this paper, we present an evaluation of radiation damage in 4H-SiC under high forward and reverse bias by means of TCAD simulations. At first we verify the accuracy of the simulation framework from Global TCAD Solutions [6] by comparing the achieved results for a silicon sensor to measurement data and established simulation tools. Afterwards, we focus on recreating measurements of 4H-SiC by utilizing the existing radiation damage model [5]. Qualitatively, good matches are achieved and the simulation results allow us to hypothesize possible causes for the observed phenomena. This publication is structured in the following fashion: We provide some background information in Section 2, describe the simulations and show the achieved results in Section 3 and conclude the paper in Section 4.

2. Background

Silicon carbide (SiC) is a wide band gap material that is heavily deployed in power electronics. It can crystallize in different atomic arrangements, called polytypes, whereas 4H is most commonly used in industry (band gap energy $E_g = 3.285\,\mathrm{eV}$ at $0\,\mathrm{K}$ [7]). Due to its high charge carrier mobility and

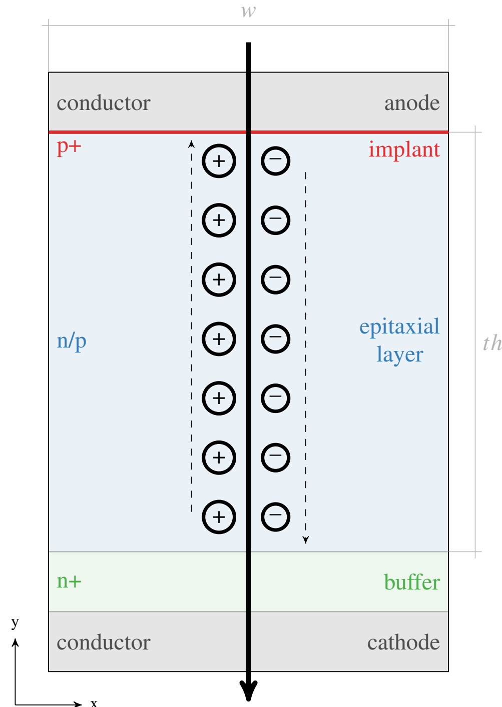

Figure 1: Structure of a pin-diode based particle detector. Impinging particles (➔) generate electron/hole pairs, which then drift, due to the potential gradient inside the device, towards the cathode/anode (- - ➤).

thermal conductivity, it is a very good alternative to the currently established silicon.

The most basic particle detectors are reverse biased pin-diodes. Electron-hole pairs are generated by an impinging particle in the space charge region and are, due to the high electric field, immediately drawn towards the cathode (electrons) resp. anode (holes) (see Fig. 1). According to the Shockley-Ramo theorem [8, 9] this drift induces a signal that can be measured.

For detection purposes the wide band gap of 4H-SiC is not solely advantageous as fewer charge carriers are generated per unit distance. In the case of a minimum ionizing particle (MIP), the overall amount is in the range of 55 to 57 electron-hole pairs per µm [10]. Increasing the device thickness (*th* in Fig. 1) and, therefore, the distance of the particle inside the active volume would strengthen the signal. However, the achievable layer thicknesses are still constrained by the limitations in growing high-quality epitaxial layers.

Consequently, sophisticated electronics is required to amplify and shape the signals before post-processing.

Further constraints on the device thickness are defined by the high intrinsic doping. In the best case impurity concentrations of approximately $10^{14}\,\mathrm{cm}^{-3}$ are currently achieved in industry, which results in an increased full depletion and operational voltage compared to silicon. Thus, for available technologies approximately 300 V to 400 V reverse bias is required to fully deplete a 50 µm thick device. Even though 4H-SiC has a very high breakdown field strength, such high voltage values imply further design challenges such as the need for guard structures and proper isolation.

To characterize the behavior of particle detectors, three measurements are commonly conducted in high energy physics as a function of the bias voltage: current (I-V), capacitance (C-V), and charge collection efficiency (CCE). I-V measurements for backward bias determine the dark current, which limits the detection sensitivity. In 4H-SiC the thermal charge carrier generation is, however, so minimal that the current stays below 1 pA and is limited in the lab by leakage paths and the measurement setup resolution. The current for forward bias helps to classify the radiation damage, as described in the next section. C-V measurements are used to evaluate the space charge region (active volume of the device), which can be used to extract the electrically active doping. Finally, the CCE is used to describe which share of the deposited charge can be collected. For this purpose, the current signal induced in a detector in response to a particle hit is recorded and integrated over time. This value is then divided by the value achieved with a reference detector, in general a defect free sample at high reverse bias.

The impact of radiation on 4H-SiC has been investigated by measurements in the past with varying results. Overall, carbon vacancies, i.e., missing carbon atoms in the lattice, are the cause of the most prominent charge carrier traps $\mathrm{Z}_{1,2}$ and $\mathrm{EH}_{6,7}$. While the former is close to the conduction band [11], the latter is located in the middle of the band gap [12, 13]. In addition to the energy level, the type of the trap (donor or acceptor) and the cross sections for electrons (σ_{e}) and holes (σ_{h}), i.e., the probability of a respective charge carrier entering the trap, are of importance. Unfortunately, the corresponding values in the literature still show a considerable spread, making a proper selection very challenging. Gaggl *et al.* [5] recently presented an analysis of the available parameters and condensed them into a TCAD radiation model for 4H-SiC.

In this paper we are going to evaluate the predictions of TCAD simu-

lations using this model by comparing the results to I-V, C-V, and CCE measurements reported by Gsponer *et al.* [1]. The authors measured 4H-SiC pin-diode detectors that were irradiated at the TRIGA Mark II reactor at the Atominstitut in Vienna [14] with 1 MeV equivalent neutron fluences between $10^{14}\,\mathrm{n_{eq}/cm^2}$ and $10^{16}\,\mathrm{n_{eq}/cm^2}$. The measurements revealed the surprising fact that the capacitance, which should change due to the varying width of the space charge region, stays constant in forward and reverse bias conditions (cp. Fig. 4a). In addition, the diodes can be forward biased with more than 1 kV without showing significant conductance (cp. Fig. 5a), although undamaged devices start conducting at around 2 V.

3. Simulations

In this section, we present the TCAD simulation results, which were achieved by Synopsys® Sentaurus [15] in version 2023.09 and the simulation framework from Global TCAD Solutions (GTS) [6] in version 2024.03 Build 25. Since we are using the latter for the first time in radiation damage simulations we start with an evaluation of the achieved accuracy by analyzing a silicon diode and comparing the results to Sentaurus simulations (based on the investigations by Schwandt *et al.* [16]). Afterwards we turn to simulations of 4H-SiC.

3.1. Verification of Silicon

For the simulations of silicon, we used the Hamburg Penta Trap Model (HPTM) [16]. As we slightly simplified the structure of the investigated device, especially the doping profiles, our results are not directly comparable to the results published by Schwandt *et al.* [16]. In detail a 1 µm wide (x-direction, w in Fig. 1) and 200 µm thick (y-direction, th in Fig. 1) 2D model of a pin-diode was used. We introduced a Boron p-type bulk doping with a concentration of $3.0 \times 10^{12}\,\mathrm{cm^{-3}}$ and Gaussian-distributed doping profiles for the p+ (Boron, top, $N_\mathrm{A} = 1.0 \times 10^{19}\,\mathrm{cm^{-3}}, \sigma = 1\,\mu\mathrm{m}$) implants and n+ buffer (Phosphorus, bottom, $N_\mathrm{D} = 1.0 \times 10^{19}\,\mathrm{cm^{-3}}, \sigma = 1\,\mu\mathrm{m}$). The diode was contacted at top and bottom by an Aluminum pad.

The simulation of the particle hit was carried out in a three step procedure: (1) The reverse bias was ramped down to -1 kV and the device characteristics were extracted at specific voltage values. (2) These conditions were taken as starting point for a short transient simulation in order to achieve mostly stable values (negligible numerical oscillation can not be avoided).

(3) The particle hit itself was added to the simulations using the heavy ion model. The particle entered in the middle of the device ($x = 0.5\,\mu\text{m}$) heading in the $-y$ - direction having a spatial Gaussian profile with $\sigma = 150\,\text{nm}$. We introduced a regular grid with 11 grid lines in x-direction (separation 100 nm), as preceding investigations revealed this as sufficient for accurate results. In the y-direction the grid was gradually refined from the middle of the device towards the contacts, with overall 400 grid lines, resulting in a maximum separation of 1.4 µm and a minimal separation of 10 nm. For unknown reasons, we were unable to run the simulations in GTS at room temperature. Only after turning the temperature down to 254 K the simulations converged. The cause for this upset is still under investigation.

The simulation results of GTS fit qualitatively well to results achieved by simulations in Sentaurus (see Fig. 2). However, also differences, especially in regard to the radiation dose, were observed. For example, almost identical capacitance values were achieved but for different fluences. In fact, scaling the latter by a factor of 0.3 led to a very good match (see Fig. 2a). The leakage current increases appropriately with higher particle flux (see Fig. 2b), although the simulations quantitatively do not match perfectly. For the CCE GTS fails to predict the decrease for fluences bigger than $3 \times 10^{15}\,\text{cm}^{-2}$ and a bias voltage smaller than $-400\,\text{V}$. In fact a misleading increase of the CCE is visible.

In some cases GTS outperforms Sentaurus: For high reverse bias and neutron fluences above $3 \times 10^{15}\,\text{n}_{\text{eq}}/\text{cm}^2$ the latter predicts an increase of the device's capacitance, which does not match the measurement results in [16]. Furthermore, the current shows some kind of dent, i.e., a slower increase followed by a steeper one at a bias voltage V of $-400\,\text{V} < V < -200\,\text{V}$. Such effects are not visible with GTS.

A key advantage of simulations compared to measurements is the ability to look inside the device. In Fig. 3 we show the simulated electric field across a reverse biased diode. Clearly visible is a double peak structure, whereat the field in the middle is almost zero. This can be explained by bulk traps that bind the majority charge carriers (electrons close to the cathode and holes close to the anode) and thus create a (quasi-stationary) space charge.

Although no perfect match among the tools was achieved, we conclude that the GTS framework is viable to provide qualitative trends in radiation damage. The quantitative differences can be, partially, explained by deviating implementations of the respective algorithms in each tool.

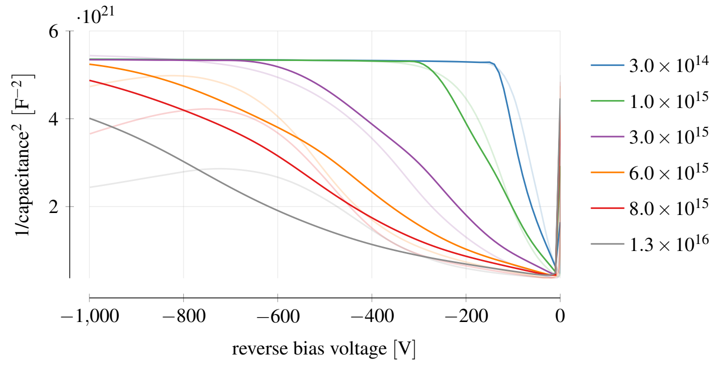

(a) capacitance (C-V)

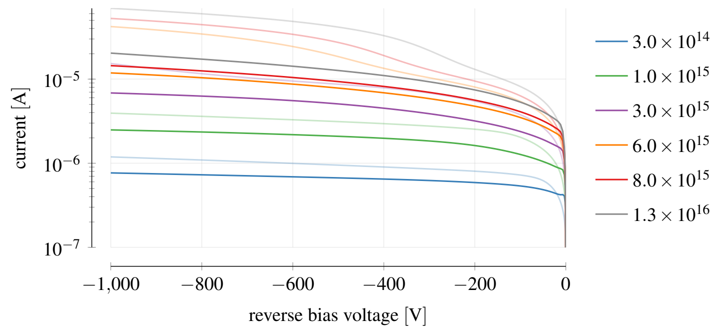

(b) current (I-V)

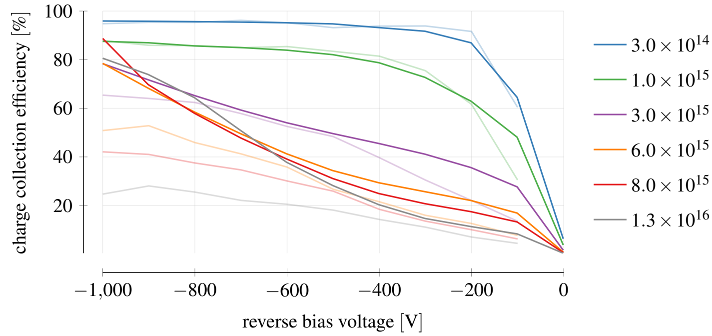

(c) charge collection efficiency (CCE)

Figure 2: Simulations of a silicon pin-diode for fluences from $3 \times 10^{14}\,\mathrm{n_{eq}/cm^2}$ to $1.3 \times 10^{16}\,\mathrm{n_{eq}/cm^2}$. Solid lines represent the simulation results from GTS and opaque lines those from Sentaurus. For a better fit, the fluences in the GTS simulations of the capacitance were scaled with a factor of 0.3.

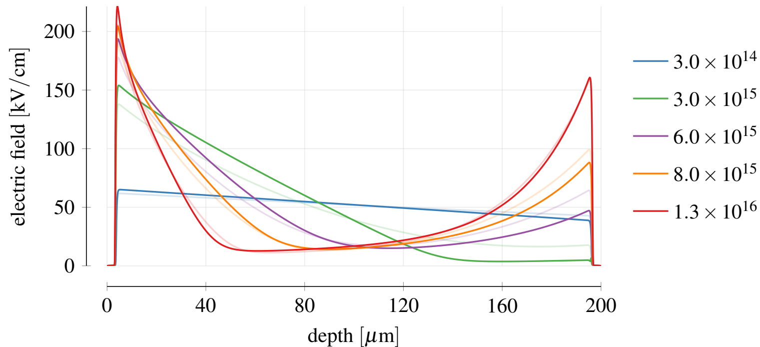

Figure 3: Electric field along the silicon diode from anode (0 µm) to cathode (200 µm) in GTS at a reverse bias of 1 kV for fluences from $3 \times 10^{14}\,\mathrm{n_{eq}/cm^2}$ to $1.3 \times 10^{16}\,\mathrm{n_{eq}/cm^2}$.

3.2. 4H-SiC Radiation Simulations

After verifying the silicon results, we turn now to a 4H-SiC diode. The respective measurements of C-V, I-V and CCE are shown in Fig. 4a, Fig. 5a and Fig. 7a. For the simulations we use the parameters in Table 1, which represent a simplified version of the model used to investigate radiation damage with Sentaurus [5].

We again simulated a 1 µm wide pin-diode but this time changed the thickness to 50 µm (y-direction, *th* in Fig. 1) due to the increased n-type bulk doping of $1.5 \times 10^{14}\,\mathrm{cm^{-3}}$. The Gaussian-distributed doping profiles for the p+ (Acceptor, top, $N_\mathrm{A} = 1.0 \times 10^{17}\,\mathrm{cm^{-3}}, \sigma = 50\,\mathrm{nm}$) implants and n+ buffer (Donor, bottom, $N_\mathrm{D} = 1.0 \times 10^{17}\,\mathrm{cm^{-3}}, \sigma = 1\,\mathrm{\mu m}$) were also changed. The diode was contacted with generic conductors at top and bottom. In order to assure convergence of the simulations we had to add artificial charge carriers via optical generation and slightly adapt the simulation grid for each

Table 1: 4H-SiC radiation damage simulation model [5]. $\sigma_\mathrm{e,h}$ denote the electron/hole cross section, E_C the conduction band energy and g_int the introduction rate.

defect	type	energy	g_int [cm^{-1}]	σ_e [cm^2]	σ_h [cm^2]
$Z_{1,2}$	acceptor	$E_\mathrm{C} - 0.67\,\mathrm{eV}$ [a]	5.0 [b]	2×10^{-14} [a]	3.5×10^{-14} [a]
$EH_{6,7}$	donor [c]	$E_\mathrm{C} - 1.6\,\mathrm{eV}$ [d,e]	1.6 [b]	9×10^{-12} [e]	3.8×10^{-14} [d,e]
EH_4	acceptor	$E_\mathrm{C} - 1.03\,\mathrm{eV}$ [f,g]	2.4 [b]	5×10^{-13} [g]	5.0×10^{-14} [g]

[a] [11] [b] [17] [c] [18] [d] [12] [e] [13] [f] [19] [g] [20]

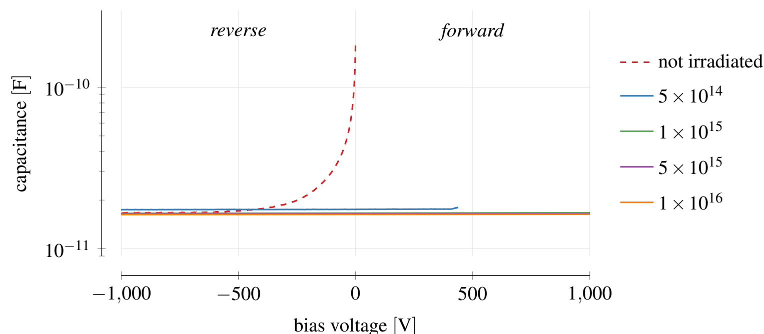

(a) measurements [1]

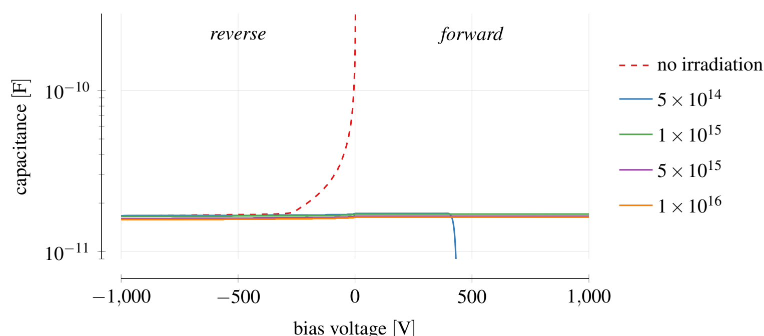

(b) GTS simulations

Figure 4: Capacitance-voltage (C-V) characteristics of a 4H-SiC diode for fluences from $5 \times 10^{14}\,\mathrm{n_{eq}/cm^2}$ to $1 \times 10^{16}\,\mathrm{n_{eq}/cm^2}$. The rapid decrease in the simulated capacitance for a fluence of $5 \times 10^{14}\,\mathrm{n_{eq}/cm^2}$ near 500 V forward bias is due to the onset of conductance (cp. Fig. 5b).

analysis.

The C-V, I-V and CCE simulation results are shown in Fig. 4b, Fig. 5b and Fig. 7b, respectively. For the capacitance the match between measurements and simulations (simply scaled to the dimensions of the actual detector) is extraordinary. The decrease of the capacitance for increasing reverse bias vanishes completely. Instead, it stays at a constant low value, which only slightly increases at large current densities in forward bias. For a fluence of $5 \times 10^{14}\,\mathrm{n_{eq}/cm^2}$ the capacitance even becomes negative, which denotes the onset of conductance (cp. Fig. 5b).

The I-V simulation results in Fig. 5b differ significantly from the measurements for reverse bias. This is a result of the very low leakage current that can be numerically calculated but is impossible to determine experimentally

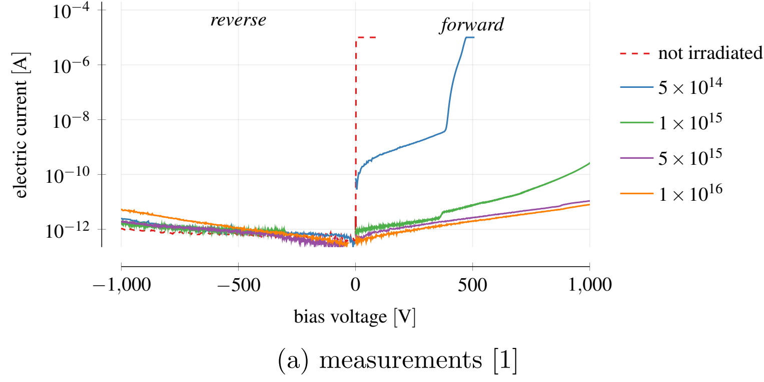

(a) measurements [1]

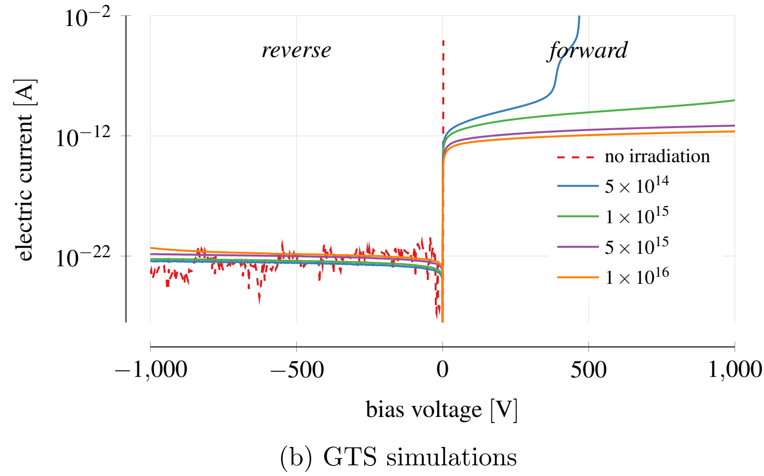

(b) GTS simulations

Figure 5: Current-voltage (I-V) characteristics of a 4H-SiC diode for fluences from $3 \times 10^{14}\,\mathrm{n_{eq}/cm^2}$ to $1.3 \times 10^{16}\,\mathrm{n_{eq}/cm^2}$.

in the lab, as edge/surface effects and other leakage paths quickly dominate. Both results, however, agree in the fact that the irradiation has little impact on the dark current.

For forward bias, the surprising decrease of conductance with radiation is clearly visible in the simulations. The respective electric field shown in Fig. 6 highlights the differences to the reverse bias simulations for silicon discussed earlier and allows, for the first time, a qualitative explanation for this phenomenon. Although, again, field peaks at both sides of the pin-diode are visible, the field drops in between below zero. Our explanation is that injected charge carriers get trapped near their respective contact, forming effectively a space charge region. The resulting electric field hinders electrons

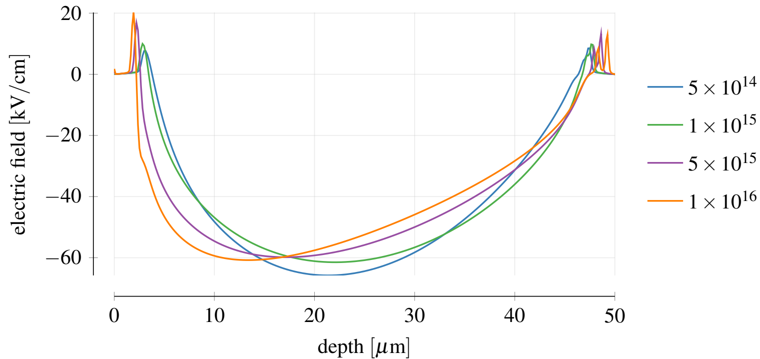

Figure 6: Electric field along the 4H-SiC diode from anode (0 μm) to cathode (50 μm) in GTS for a forward bias of 200 V and various fluences in n_{eq}/cm^2.

and holes from entering the device, resulting in the very low conductance. At a sufficient forward bias all traps are filled, i.e., the field reaches a maximum. Any further increase of the bias voltage can not be compensated by space charge any more, resulting in a significant increases of the recombination current.

The charge collection efficiency in Fig. 7b finally shows a quantitative good agreement, especially for high fluences. For low radiation doses the impact of the damage is slightly underestimated, i.e., the CCE values are too high. The results show that even at the lowest flux investigated a reverse bias of 1 kV it is not sufficient any more to collect all the deposited charges. This can be explained by the additional traps that either act as recombination centers or release captured charge carriers only after the signal has faded, making them disappear in the noise.

4. Conclusion

In this paper we presented a comparison of technology computer aided design (TCAD) simulations run with Sentaurus and the simulation framework from Global TCAD Solutions (GTS) against previously published simulation and measurement results of radiation damage in Si and SiC. Overall, the available capacitance, electric current and charge collection efficiency data were approximated closely. Based on the electric field deep inside the devices we were able to provide, for the first time, an explanation for the reduced conductance of radiated diodes in forward bias. In detail, trapped

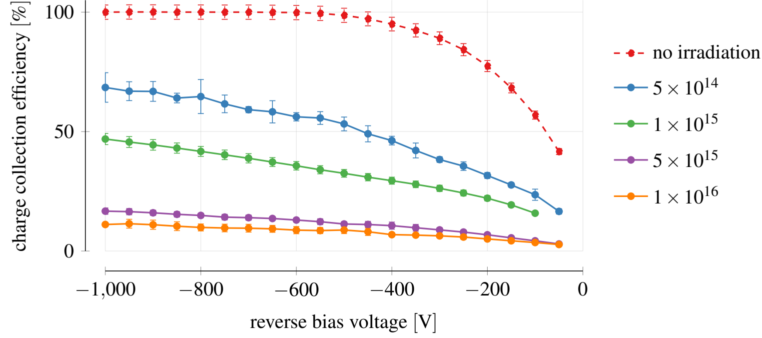

(a) measurements [1]

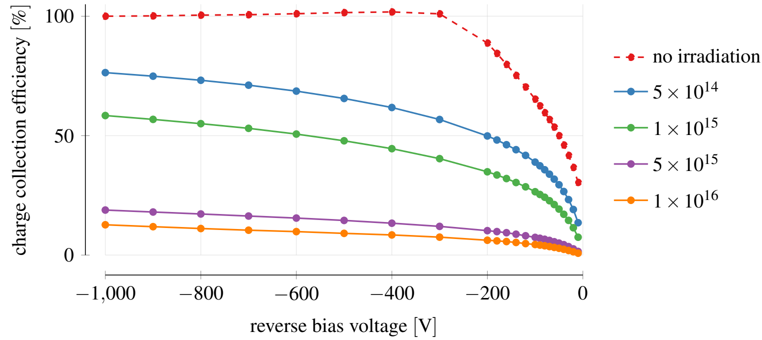

(b) GTS simulations

Figure 7: Charge collection efficiency (CCE) of a 4H-SiC diode for fluences from $5 \times 10^{14}\,\mathrm{n_{eq}/cm^2}$ to $1 \times 10^{16}\,\mathrm{n_{eq}/cm^2}$. The simulations predict less reduction than seen by measurements.

majority charge carriers effectively create a space charge region that hinders further charge carriers from entering the device.

In hindsight, our simulations show that the GTS framework is a suitable tool for radiation damage simulations in 4H-SiC. Our goal is to use such investigations in the development of next generation particle detector systems, i.e., to estimate the performance degradation during a life cycle. In cooperation with GTS we also plan to further improve the capabilities of the simulation framework, as occasionally nonphysical results have been achieved. Additional future research will be focused on a more thorough analysis of the introduced trap parameters, i.e., energy level, type, and cross-section, as literature values show large deviations.

References

[1] A. Gsponer, P. Gaggl, J. Burin, R. Thalmeier, S. Waid, T. Bergauer, Neutron radiation induced effects in 4H-SiC PiN diodes, Journal of Instrumentation 18 (11) (2023) C11027. doi:10.1088/1748-0221/18/11/C11027.

[2] A. Siddiqui, M. Usman, Radiation tolerance comparison of silicon and 4H–SiC Schottky diodes, Materials Science in Semiconductor Processing 135 (2021) 106085. doi:https://doi.org/10.1016/j.mssp.2021.106085.

[3] S. Ganiyev, N. Muridan, N. F. Hasbullah, Y. Abdullah, Electrical simulation of Ni/4H-SiC Schottky diodes before and after low energy electron radiation, in: 2015 IEEE Regional Symposium on Micro and Nanoelectronics (RSM), 2015, pp. 1–4. doi:10.1109/RSM.2015.7354995.

[4] Y. Sun, Z. Hu, H. Zhang, P. Gong, G. Zhong, L. Hu, G. Gorini, G. Croci, X. Tang, Investigation of the Performance Degradation of 4H-SiC Neutron Detectors Using MCNP and TCAD, IEEE Sensors Journal 24 (4) (2024) 4432–4441. doi:10.1109/JSEN.2023.3345407.

[5] P. Gaggl, J. Burin, A. Gsponer, S.-E. Waid, R. Thalmeier, T. Bergauer, TCAD modeling of radiation-induced defects in 4H-SiC diodes, Nuclear Instruments and Methods in Physics Research Section A: Accelerators, Spectrometers, Detectors and Associated Equipment 1070 (2025) 170015. doi:https://doi.org/10.1016/j.nima.2024.170015.

[6] GTS Framework (2025) [cited 22.01.2025].
URL https://www.globaltcad.com/products/gts-framework/

[7] J. Freitas Jr, Photoluminescence spectra of SiC polytypes, Properties of Silicon Carbide, Ed. GL Harris//EMIS Datareviews Series (13) (1995) 29–41.

[8] W. Shockley, Currents to Conductors Induced by a Moving Point Charge, Journal of Applied Physics 9 (10) (1938) 635–636. doi:10.1063/1.1710367.

[9] Z. He, Review of the Shockley–Ramo theorem and its application in semiconductor gamma-ray detectors, Nuclear Instruments and Methods

in Physics Research Section A: Accelerators, Spectrometers, Detectors and Associated Equipment 463 (1) (2001) 250–267. doi:https://doi.org/10.1016/S0168-9002(01)00223-6.

[10] A. Gsponer, M. Knopf, P. Gaggl, J. Burin, S. Waid, T. Bergauer, Measurement of the electron–hole pair creation energy in a 4H-SiC p-n diode, Nuclear Instruments and Methods in Physics Research Section A: Accelerators, Spectrometers, Detectors and Associated Equipment 1064 (2024) 169412. doi:https://doi.org/10.1016/j.nima.2024.169412.

[11] P. B. Klein, Identification and Carrier Dynamics of the Dominant Lifetime Limiting Defect in n $^-$ 4H-SiC Epitaxial Layers: Dominant Lifetime Limiting Defect in n $^-$ 4H-SiC Epitaxial Layers, physica status solidi (a) 206 (10) (2009) 2257–2272. doi:10.1002/pssa.200925155.

[12] M. L. Megherbi, F. Pezzimenti, L. Dehimi, A. Saadoune, F. G. Della Corte, Analysis of the Forward I–V Characteristics of Al-Implanted 4H-SiC p-i-n Diodes with Modeling of Recombination and Trapping Effects Due to Intrinsic and Doping-Induced Defect States, Journal of Electronic Materials 47 (2) (2018) 1414–1420. doi:10.1007/s11664-017-5916-8.

[13] J. Zhang, L. Storasta, J. P. Bergman, N. T. Son, E. Janzén, Electrically Active Defects in n -Type 4H–Silicon Carbide Grown in a Vertical Hot-Wall Reactor, Journal of Applied Physics 93 (8) (2003) 4708–4714. doi:10.1063/1.1543240.

[14] P. Gaggl, T. Bergauer, M. Göbel, R. Thalmeier, M. Villa, S. Waid, Charge collection efficiency study on neutron-irradiated planar silicon carbide diodes via UV-TCT, Nuclear Instruments and Methods in Physics Research Section A: Accelerators, Spectrometers, Detectors and Associated Equipment 1040 (2022) 167218. doi:https://doi.org/10.1016/j.nima.2022.167218.

[15] Synopsys Sentaurus TCAD Framework (2025) [cited 22.01.2025].
URL https://www.synopsys.com/manufacturing/tcad/framework.html

[16] J. Schwandt, E. Fretwurst, E. Garutti, R. Klanner, C. Scharf, G. Steinbrueck, A new model for the TCAD simulation of the silicon damage by

high fluence proton irradiation, in: 2018 IEEE Nuclear Science Symposium and Medical Imaging Conference Proceedings (NSS/MIC), 2018, pp. 1–3. doi:10.1109/NSSMIC.2018.8824412.

[17] P. Hazdra, V. Záhlava, J. Vobecký, Point Defects in 4H–SiC Epilayers Introduced by Neutron Irradiation, Nuclear Instruments and Methods in Physics Research Section B: Beam Interactions with Materials and Atoms 327 (2014) 124–127. doi:10.1016/j.nimb.2013.09.051.

[18] T. Hornos, A. Gali, B. G. Svensson, Large-Scale Electronic Structure Calculations of Vacancies in 4H-SiC Using the Heyd-Scuseria-Ernzerhof Screened Hybrid Density Functional, Materials Science Forum 679–680 (2011) 261–264. doi:10.4028/www.scientific.net/MSF.679-680.261.

[19] C. Hemmingsson, N. T. Son, O. Kordina, J. P. Bergman, E. Janzén, J. L. Lindström, S. Savage, N. Nordell, Deep Level Defects in Electron-Irradiated 4H SiC Epitaxial Layers, Journal of Applied Physics 81 (9) (1997) 6155–6159. doi:10.1063/1.364397.

[20] G. Alfieri, E. V. Monakhov, B. G. Svensson, M. K. Linnarsson, Annealing Behavior between Room Temperature and 2000 °C of Deep Level Defects in Electron-Irradiated n-Type 4H Silicon Carbide, Journal of Applied Physics 98 (4) (2005) 043518. doi:10.1063/1.2009816.